Catalysis Today 141 (2009) 234–241

Contents lists available at ScienceDirect

Catalysis Today

journal homepage: www.elsevier.com/locate/cattod

Selective epoxidation of dimethyl maleate to *cis*-epoxydimethyl succinate over solid acid catalysts

M. Bhagiyalakshmi, J. Herbert Mabel, S. Vishnupriya, M. Palanichamy, V. Murugesan *

Department of Chemistry, Anna University, Chennai 600025, India

ARTICLE INFO

Article history:
Available online 4 September 2008

Keywords:
Epoxidation
cis-Epoxydimethyl succinate
Dimethyl tartrate
Dimethyl maleate
HPW supported Al-MCM-41

ABSTRACT

Al-MCM-41 (Si/Al = 50), Al-MCM-41 (50) supported phosphotungstic acid (HPW) and Hβ supported HPW were prepared and characterized using XRD, FT-IR, TPD (pyridine) and ^{31}P MAS-NMR. Epoxidation of dimethyl maleate (DMM) with tert-butylhydroperoxide (TBHP) over these catalysts was studied at 60, 80, 100 and 120 °C. *cis*-Epoxydimethyl succinate (CEMS) and dimethyl tartrate (DMT) were the major and minor products, respectively. Forty percent HPW-Hβ zeolite was found to be more active than 20% HPW-Al-MCM-41 (50), 40% HPW-Al-MCM-41 (50), 20% HPW-Hβ zeolite and Hβ zeolite. The active sites for this reaction were ascribed to Lewis acid sites present in these catalysts. Feed ratios (DMM:TBHP) of 1:5 and 1:10 were found to give high selectivity of CEMS at maximum DMM conversion. The formation of CEMS without its trans isomer in a single step epoxidation of DMM is the salient feature of this study. The leaching of HPW from the support was not observed in this study.

1. Introduction

Epoxidation of alkenes can be accomplished by hydrogen peroxide in combination with a variety of catalysts, the choice of which is often decided by the structure of the oxidizable substrate [1]. Epoxidation of α,β-unsaturated acid using reagents such as peroxybenzoic acid or peroxyacetic acid is generally very slow due to electron withdrawing effect of the carboxyl group directly attached to the ethylenic double bond [2]. In such cases, compounds of metals such as W, Mo, V, Os, Ti, Zr, Th, Nb, Ta, Cr, Ru and Se have been generally employed as catalysts, in particular W compounds are effective for the conversion of α,β-unsaturated acid to the corresponding *cis*-epoxide [3]. It was reported that Lewis acid sites are the active sites in these catalysts. Maleic acid epoxidation using hydrogen peroxide with sodium tungstate has been well studied in homogeneous liquid phase yielding *cis*-epoxysuccinic acid [4]. Realizing the need of Lewis acid sites, solid materials such as aluminium oxide (α-Al_2O_3) and ferric oxide (Fe_2O_3), which are practically insoluble in aqueous medium, were also used as catalyst for the epoxidation of maleic anhydride to *cis*-epoxysuccinic acid [5].

The epoxidation of maleic acid over tungstate modified Dowex resin catalysts was also reported [6]. But there are problems like leaching of tungstate from the resin and maintaining pH of maleic acid. Considering these problems, the present study focussed the epoxidation of dimethyl maleate (DMM) with tert-butylhydroperoxide (TBHP) over Al-MCM-41 (50) supported HPW, Hβ and Hβ supported HPW catalysts. Although Bronsted and Lewis acid sites are present in these catalysts, Lewis acid sites are important for activation of dimethyl maleate. The principally aimed product was *cis*-epoxydimethyl succinate (CEMS). This kind of substituted epoxide has commercial utility as plasticizers and stabilizer for polyvinyl chloride [7] and precursor for epoxy resin [8]. The main purpose of the present investigation is to extend the idea for the epoxidation of α,β-unsaturated ester to obtain *cis*-epoxy succinic ester using Al-MCM-41 (50) supported HPW, Hβ and Hβ supported HPW catalysts.

2. Experimental

2.1. Synthesis of catalysts

Hydrothermal crystallization procedure of Beck et al. [9] was adopted for the preparation of Al-MCM-41 (Si/Al = 50) molecular sieve. In a typical synthesis, 10.6 g of sodium silicate nanohydrate (Merck) in 80 mL deminerlized water was combined with 0.6 g aluminium sulphate (Merck). It was then acidified with 1 M H_2SO_4 to bring down the pH to 10.5 under vigorous stirring. After 30 min stirring, an aqueous solution of cetyltrimethylammonium bromide (CTAB) (Merck) was added and the surfactant-silicate mixture was

* Corresponding author. Tel.: +91 44 2220 3144; fax: +91 44 2235 0397.
E-mail address: v_murugu@hotmail.com (V. Murugesan).

0920-5861/$ – see front matter © 2008 Elsevier B.V. All rights reserved.
doi:10.1016/j.cattod.2008.07.029

stirred for further 30 min at room temperature. The resultant gel was autoclaved and heated at 170 °C for 12 h. The solid product obtained was filtered and dried at 80 °C in air. The sample was then calcined at 550 °C for 5 h in a muffle furnace to expel the template. Al-MCM-41 (50) supported phosphotungstic acid (20 and 40 wt.%) was obtained by mixing 1.0 g Al-MCM-41 (50) in 10 mL methanol containing 0.2 or 0.4 g HPW at room temperature for 24 h [10,11]. The resultant mixture was dried at 100 °C and calcined at 200 °C for 2 h [12]. The supported catalysts are hereafter abbreviated as 20 and 40% HPW-Al-MCM-41.

Zeolite β was purchased from Sud. Chemie India Ltd. and was converted to NH_4^+ form by ion-exchange with 0.5 M ammonium chloride solution. About 1 g of the catalyst was mixed with 20 mL ammonium chloride solution in a round-bottom flask fitted with a reflux condenser. The solution was stirred magnetically for 3 h; the content of the flask was cooled and filtered. The residue was dried at 100 °C for 6 h in an air oven and calcined at 550 °C for 6 h. The same procedure was repeated thrice. After calcination, the ammonium chloride exchanged zeolite gave protonic form of β zeolite. Hβ supported HPW catalyst was prepared by impregnation of HPW (0.2 or 0.4 g) on 1 g Hβ by incipient wetness method as described above. The supported catalysts are hereafter abbreviated as 20 and 40% HPW-Hβ.

2.2. Characterisation

The powder XRD of calcined mesoporous Al-MCM-41 (50) molecular sieve was recorded on a diffractometer (Stereoscan) using nickel-filtered CuKα radiation as the X-ray source and liquid nitrogen cooled germanium solid-state detector. The diffractograms were recorded in the 2θ range 5–60° in steps of 0.02° with a count time of 15 s at each point for Hβ zeolite and HPW-Hβ whereas for Al-MCM-41 (50) and HPW-Al-MCM-41 (50) molecular sieves the diffractograms were recorded in the 2θ range 0–50°. The formation of primary Keggin structure of HPW on Al-MCM-41 and Hβ was studied by FT-IR spectroscopy. All the spectra were recorded on a FT-IR spectrometer (Nicolet Avatar 360) using KBr pellet technique. About 15 mg of the sample was pressed using hydraulic press under a pressure 2 tons cm^{-2} into a self-supported wafer of 13 mm diameter. This pellet was used to record the infrared spectra in the range 4000–400 cm^{-1}. The pellets were scanned 50 times at 4 cm^{-1} resolution. The spectra were recorded as percentage transmittance against wave number.

^{31}P MAS-NMR spectra were recorded using solid-state NMR spectrometer (Bruker DSX-300) with a magnetic field strength of 7.04 T and a spinning rate of 8 kHz. The resonating frequency 121.5 MHz, spectral width 8 μs, recycle delay 2 s and number of transients 1043 were used for recording the spectra. Phosphoric acid was used as the reference compound. The acidity of the catalysts was determined by *in situ* DRIFT pyridine adsorption–desorption technique. The *in situ* DRIFT spectra of the samples were recorded on a FT-IR spectrometer (Nicolet Avatar 360) equipped with a high temperature vacuum chamber. Approximately 30 mg of the sample was taken in the sample holder and dehydrated at 400 °C for 6 h under vacuum (10^{-5} mbar). The sample was then cooled to room temperature and the spectrum was recorded. Then pyridine was adsorbed on the catalyst at room temperature. The physically adsorbed pyridine was removed by heating the sample at 150 °C under vacuum (10^{-5} mbar) for 30 min, cooled to room temperature and then the spectrum was recorded in the range 1700–1400 cm^{-1} (pyridine adsorption region). The number of Bronsted and Lewis acid sites was calculated by measuring the integrated absorbance of bands representing pyridinium ion formation and co-ordinatively bonded pyridine [13]. The method developed for porous materials by Emeis [14] was adopted for the determination of acidity of the catalysts. The integrated molar extinction coefficients were calculated assuming that they did not depend on the catalyst or the strength of the acid site. The following equations are used to determine the concentration of acid sites in these catalysts.

$$C_{(\text{pyridine on B sites})} = 1.88\text{IA(B)} \times R^2/W$$
$$C_{(\text{pyridine on L sites})} = 1.42\text{IA(L)} \times R^2/W$$

where C is the concentration (mmol g^{-1}) of the material, IA is the integrated absorbance of Bronsted or Lewis band (cm^{-1}), R is the radius of the catalyst disk (cm) and W is the weight of the disk (mg).

2.3. Epoxidation of dimethyl maleate with tert-butylhydroperoxide

Epoxidation of dimethyl maleate with tert-butylhydroperoxide was carried out in the liquid phase. DMM (1 mol), TBHP (1 mol) and catalyst (0.1 g) were taken in a 25 mL round-bottom flask fitted with a reflux condenser. The flask with its content was heated at different temperatures (60, 80,100 and 120 °C) in an oil bath with simultaneous magnetic stirring. In order to monitor the progress of the reaction, aliquots of the hot mixture were withdrawn at regular intervals (3, 6, 9 and 12 h). The samples were then centrifuged and the centrifugate was analysed using high performance liquid chromatography (HPLC) (Agilent1100 series) equipped with a phenomenex C18 column and Variable UV detector. The mobile phase used for this analysis was 0.1 M phosphoric acid at a flow rate of 1 mL min^{-1}. The wavelength maximum was set at 254 nm. The injection volume of the sample was 20 μL. The product identification was done by liquid chromatography coupled with mass spectrometer (LC–MS/MS) (Micromass Qualtro Ultimate Pt Waters 2695 separation module-mass lynx).

3. Results and discussion

3.1. XRD diffraction

XRD patterns of as-synthesized and calcined Al-MCM-41 (50) are similar to those already reported in the literature [15,16]. The XRD patterns of calcined Al-MCM-41 (50) exhibit an intense signal at about 1.8° due to [1 0 0] and weak signals between 2 and 4° (2θ) due to [1 1 0], [2 0 0] and [2 1 0] planes which are indexed to hexagonal lattice [9,17]. These peaks confirm the hexagonal mesophase of the material. Their d_{100} spacing calculated as per the literature procedure [16] is 37.43 while the lattice parameter (a_o) is 43.29°. The XRD patterns of calcined Al-MCM-41 (50), 20 and 40% HPW-Al-MCM-41 (50) are shown in Fig. 1A (a–c). The [1 0 0] plane reflection has been shifted to higher values of 2θ at 2.32° for 20 and 40% HPW-Al-MCM-41, which is an indication of pore size decrease illustrating maximum use of HPW to construct the Keggin phase within the pores [12]. Comparison of the XRD patterns of Al-MCM-41 (50) and 20 and 40% HPW-Al-MCM-41 (50) revealed that the mesoporous structure is rather intact even after the loading of HPW. The XRD patterns of Hβ, 20 and 40% HPW-Hβ zeolite are shown in Fig. 1B (a–c). The diffractogram of Hβ shows more intense peak about 23° (2θ) and less intense peak at 7.8° (2θ) which are similar to the data already reported for Hβ [18]. The characteristic peaks for Hβ zeolite in addition to intense peak due to HPW are seen in 20 and 40% HPW-Hβ. The intense peak at 26.4° (2θ) is due to the formation of Keggin phase of HPW on Hβ zeolite. Although the XRD patterns of 40% HPW-Hβ are similar to 20% HPW-Hβ, the intensity of 40% HPW-Hβ at 26.4° (2θ) is more than that of 20% HPW-Hβ. Hence there is a possibility for the

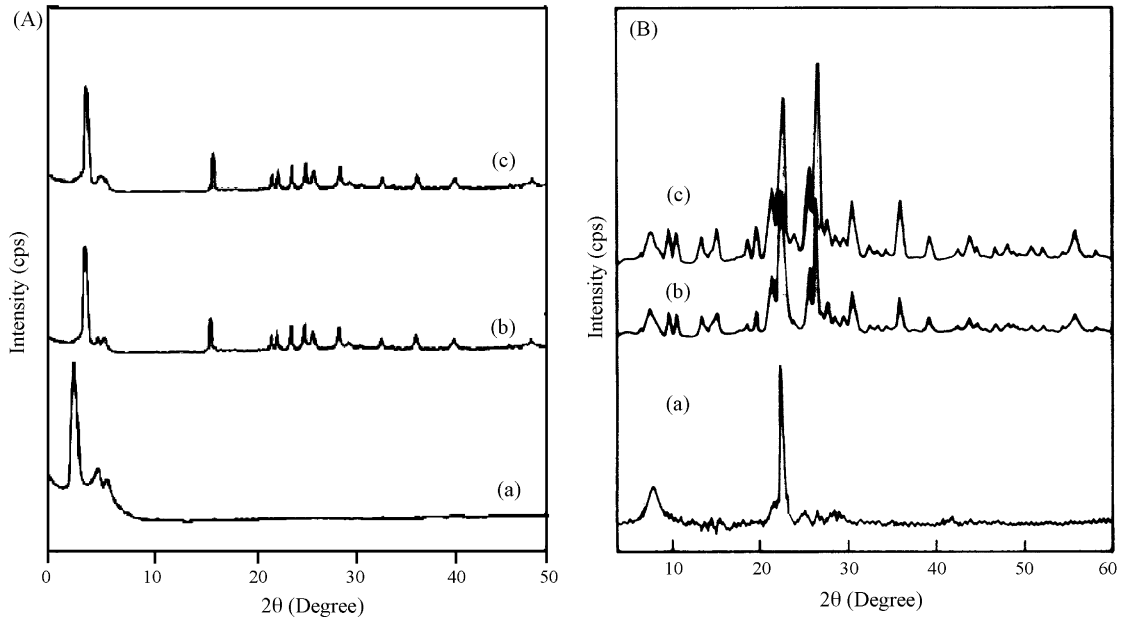

Fig. 1. XRD patterns of A: (a) Al-MCM-41 (50), (b) 20% HPW-Al-MCM-41 (50), and (c) 40% HPW-Al-MCM-41 (50); B: (a) Hβ, (b) 20% HPW-Hβ and (c) 40% HPW-Hβ.

formation of larger HPW Keggin phase in 40% HPW-Hβ than in 20% HPW-Hβ. This is also evident from the mid FT-IR spectra of 20 and 40% HPW-Hβ.

3.2. FT-IR spectra of 20 and 40% HPW-Al-MCM-41 (50)

FT-IR spectra were recorded for supported HPW catalysts in order to confirm the presence of Keggin anion in Al-MCM-41 (50). The FT-IR spectra of Al-MCM-41 (50), 20 and 40% HPW-Al-MCM-41 (50) are shown in Fig. 2a–c. The $PW_{12}O_{40}^{3-}$ Keggin ion structure consists of a PO_4 tetrahedron surrounded by four W_3O_{13} groups formed by edge sharing octahedra. These groups are connected to each other by corner-sharing oxygen [19]. The spectra revealed typical bands of Keggin absorption at 1091, 968, 896 and 802 cm^{-1}. This structure gave rise to four types of oxygen, which are responsible for the finger print bands of Keggin ion between 1200 and 700 cm^{-1}. The bands at 1080 and 984 cm^{-1} are due to P–O and W=O vibrations, respectively. The corner-shared and edge-shared vibrations of W–O–W bands occur at 892 and 800 cm^{-1}, respectively [10,20]. These spectral features remained the same irrespective of HPW loading. A gradual increase in the absorbance of W–O–W corner shared vibrations at 892 cm^{-1} is observed for Al-MCM-41 supported HPW catalysts. Hence, it may be concluded that significant amount of crystallisation of Keggin phase starts only at and above 20 wt.% loading of HPW. In addition, the peaks between 400 and 1200 cm^{-1} are assigned to SiO_4 framework vibrations. The intense peak at 1123 cm^{-1} is due to the asymmetric stretching of T–O–T groups. The symmetric stretching modes of T–O–T groups are observed around 800 cm^{-1} and the peak at 460 cm^{-1} is due to the bending modes of T–O–T. The peak at 963 cm^{-1} is assigned to the presence of defective Si–OH groups [21].

3.3. FT-IR spectra of 20 and 40% HPW-Hβ

The FT-IR spectra of 20 and 40% HPW-Hβ are shown in Fig. 2d and e. It shows similar features as that of the spectrum of 20% HPW-Al-MCM-41. But there are some variations in the low energy region with bands between 800 and 1200 cm^{-1} due to W=O, P–O and W–O–W vibrations of Keggin phase. These vibrations support the formation of Keggin phase even with 20% loading of HPW in Hβ zeolite. The intense band at about 1083 cm^{-1} is a common one for zeolite framework and P–O vibrations. The spectrum of 40% HPW-Hβ is same as that of 20% HPW-Hβ. But the intensity due to W=O vibration at 982 cm^{-1} and W–O–W vibrations at 893 and 812 cm^{-1}

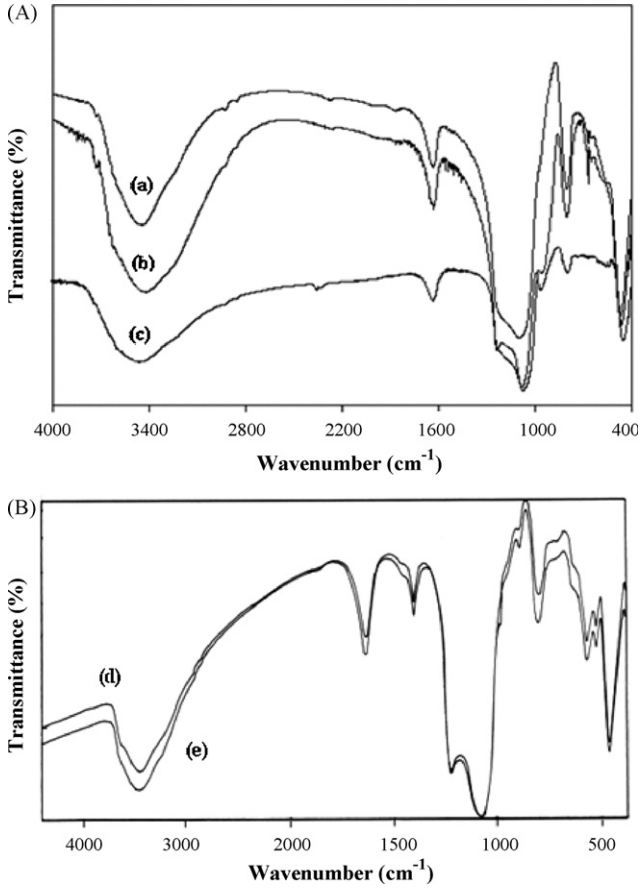

Fig. 2. FT-IR spectrum of A: (a) Al-MCM-41 (50), (b) 20% HPW-Al-MCM-41 (50), and (c) 40% HPW-Al-MCM-41 (50); B: (d) 20% HPW-Hβ, and (e) 40% HPW-Hβ.

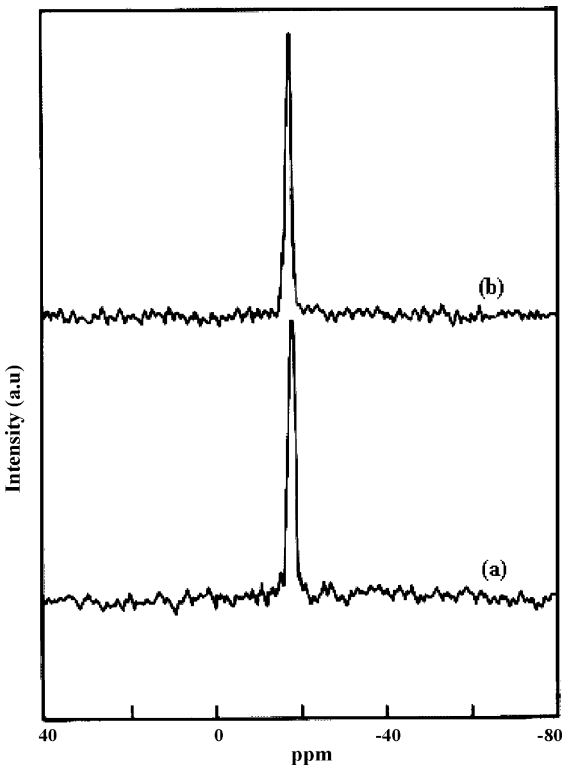

Fig. 3. ^{31}P MAS-NMR spectrum of (a) 20% HPW-Al-MCM-41 (50), and (b) 40% HPW-Al-MCM-41 (50).

appear more intense than 20% HPW-Hβ. This is due to larger Keggin phase in 40% HPW-Hβ than in 20% HPW-Hβ. This is in accordance with XRD analysis of 20 and 40% HPW-Hβ.

3.4. ^{31}P MAS-NMR spectra of 20 and 40% HPW-Al-MCM-41 (50)

The ^{31}P MAS-NMR spectra of 20 and 40% HPW-Al-MCM-41 (50) shown in Fig. 3 exhibit a sharp peak at −15.2 ppm, which is close to that of bulk HPW [10]. This indicates unambiguously that Keggin structure is retained when HPW is loaded on Al-MCM-41 (50).

Table 1
Bronsted and Lewis acidity values for pristine and supported Al-MCM-41 (50) and Hβ

Catalyst	Concentration (mmol g^{-1})		B/L ratio
	Bronsted (B) acid site	Lewis (L) acid site	
20% HPW-Al-MCM-41	0.25	0.32	0.78
40% HPW-Al-MCM-41	0.20	0.27	0.74
20% HPW-Hβ	0.36	0.43	0.84
40% HPW-Hβ	0.31	0.35	0.89
Al-MCM-41 (50)	0.12	0.18	0.66
Hβ	0.25	0.22	1.13

Desorption temperature = 150 °C.

3.5. Acidity analysis

FT-IR spectra of 20 and 40% HPW-Al-MCM-41 (50) were recorded after adsorption of pyridine followed by evacuation in the temperature range between 100 and 200 °C (Fig. 4). The peaks at 1545 and 1634 cm^{-1} are due to pyridine adsorbed on Bronsted acid sites. The peaks at 1445 and 1613 cm^{-1} are due to pyridine adsorbed on Lewis acid sites. The peak at 1490 cm^{-1} is due to pyridine adsorbed on both Bronsted and Lewis acid sites [22–26]. The concentration of Bronsted and Lewis acid sites of Al-MCM-41 (50), 20 and 40% HPW-Al-MCM-41 (50), Hβ, 20 and 40% HPW-Hβ are presented in Table 1.

3.6. Epoxidation of dimethyl maleate

Epoxidation of dimethyl maleate with tert-butyl hydroperoxide (TBHP) was carried over 20% HPW-Al-MCM-41(50), 40% HPW-Al-MCM-41(50), 20% HPW-Hβ, 40% HPW-Hβ and Hβ zeolite at 60, 80, 100 and 120 °C for 12 h. The products were found to be dimethyl tartrate (DMT) and *cis*-epoxydimethyl succinate.

3.6.1. Effect of temperature

The effect of temperature and reaction time on the yield of products are illustrated in Fig. 5a–d. The conversion of DMM over 20% HPW-Al-MCM-41 (50) increases with increase in reaction time and attains steady state at the end of 12 h at each temperature. The conversion also increases with increase in temperature from 60 to 80 °C but above this temperature the conversion decreases. Hence the optimum temperature for maximum conversion is 80 °C. The less conversion at 100 and 120 °C is due to decomposition of TBHP.

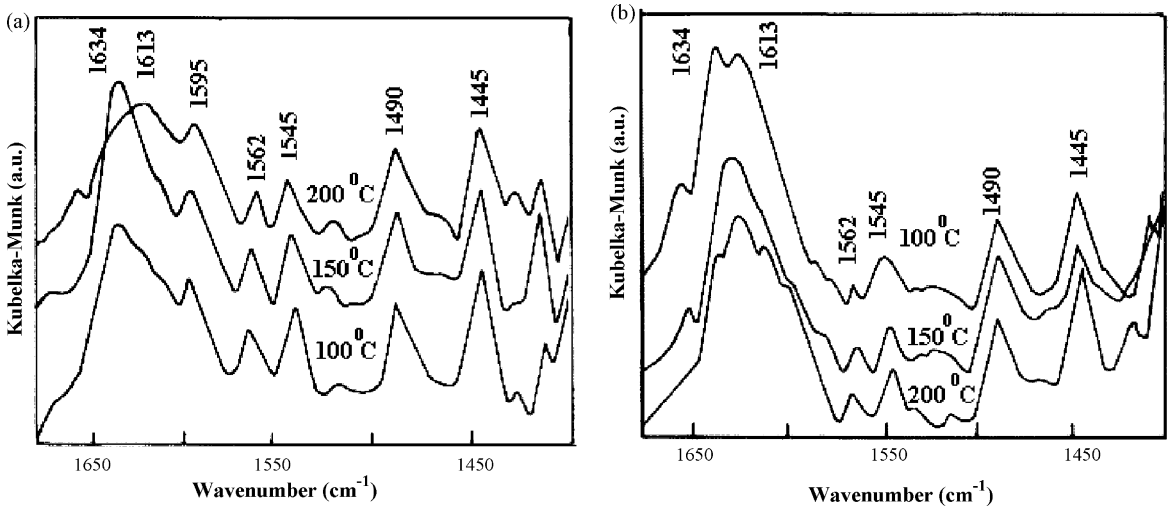

Fig. 4. Pyridine adsorbed *in situ* DRIFT spectra of (a) 20% HPW-Al-MCM-41 (50), and (b) 40% HPW-Al-MCM-41 (50).

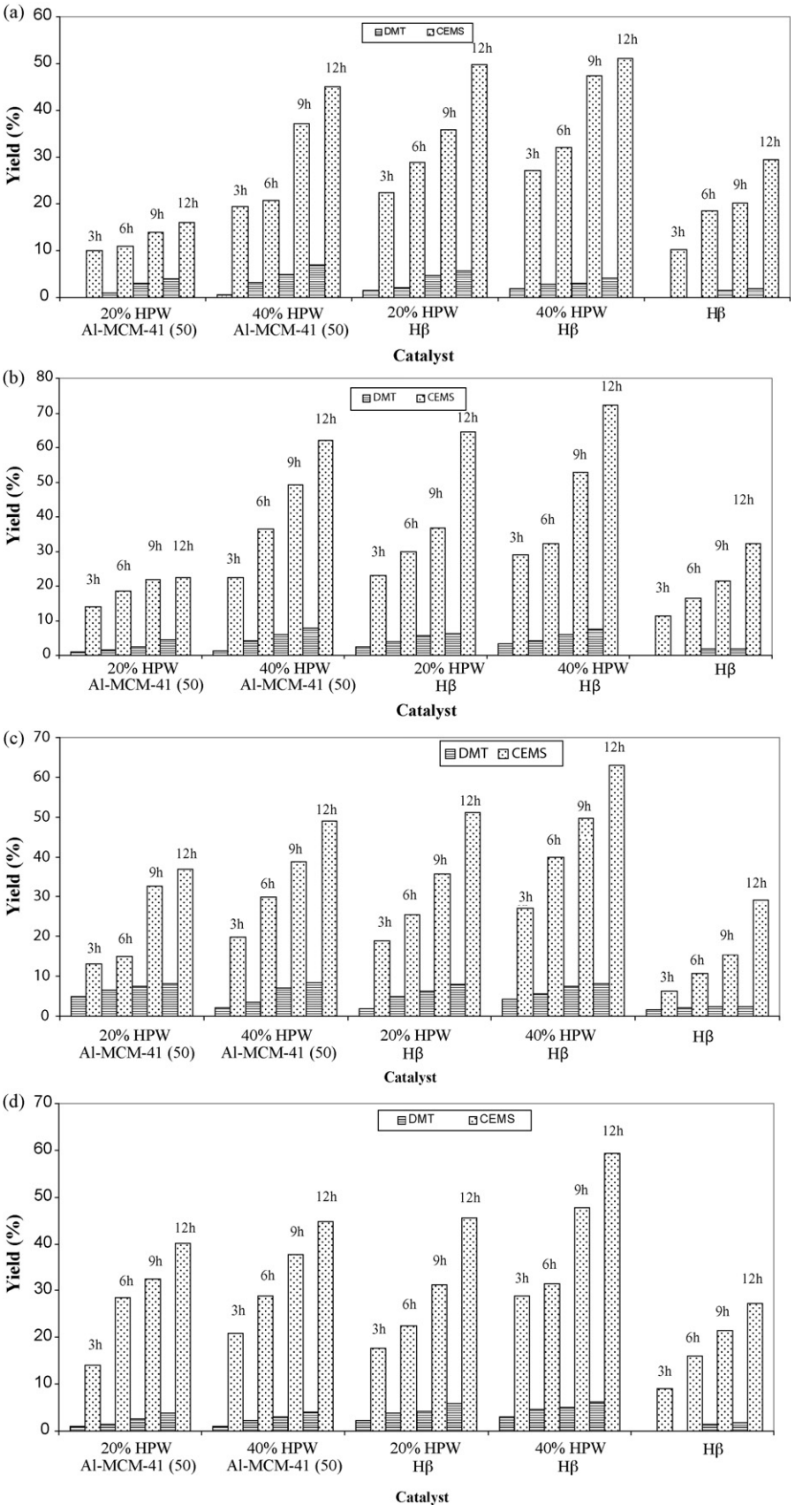

Fig. 5. (a) Effect of temperature on the yield of products: temperature 60 °C; catalyst amount 0.1 g; dimethyl maleate:TBHP molar ratio 1:2. (b) Effect of temperature on the yield of products: temperature 80 °C; catalyst amount 0.1 g; dimethyl maleate:TBHP molar ratio 1:2. (c) Effect of temperature on the yield of products: temperature 100 °C; catalyst amount 0.1 g; dimethyl maleate:TBHP molar ratio 1:2. (d) Effect of temperature on the yield of products: temperature 120 °C; catalyst amount 0.1 g; dimethyl maleate:TBHP molar ratio 1:2.

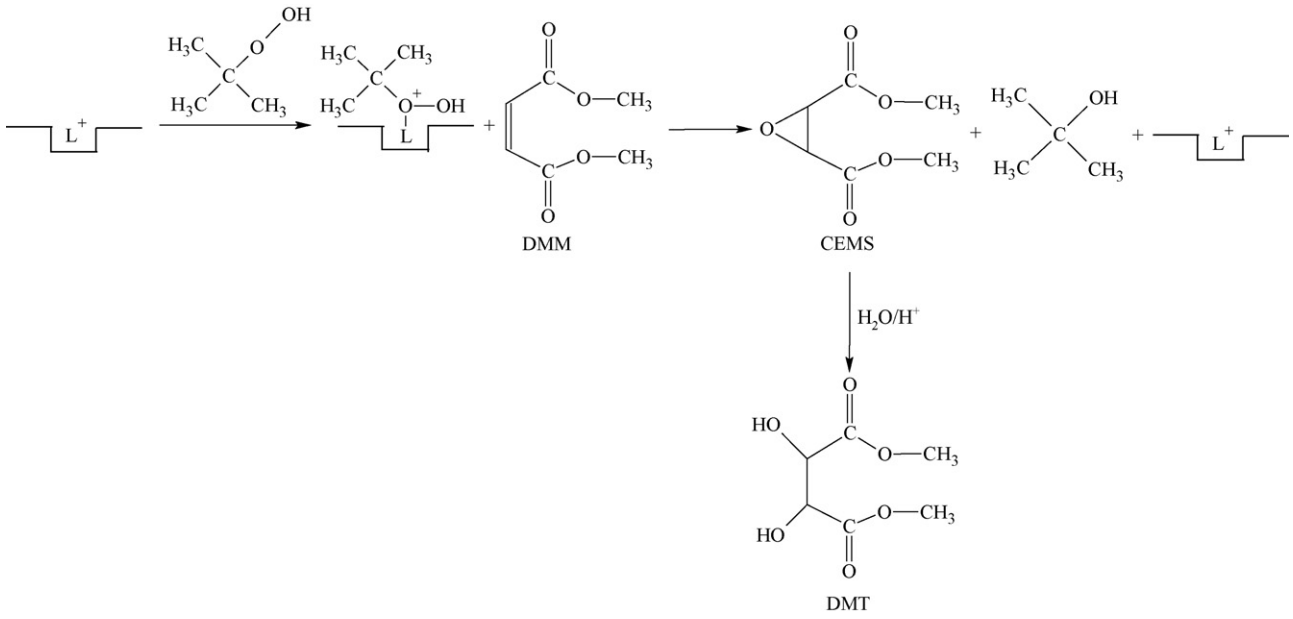

Scheme 1.

The reaction is presumed to be catalysed mainly by Lewis acid sites as shown in the reaction Scheme 1. TBHP is chemisorbed on the Lewis acid sites and the activated distant oxygen of TBHP is added to DMM across its double bond thus yielding CEMS. The insertion of oxygen across the double bond is a single step process as trans-epoxysuccinate is not observed. In addition to this principally aimed product, its hydrolysed product, namely, DMT is also obtained due to the presence of adsorbed water on the catalyst. The hydrolysis of CEMS is catalysed by Bronsted acid sites of the catalyst. The yield of DMT increases with increase in time. The conversion increases with increase in reaction time over 40% HPW-Al-MCM-41 (50). The conversion is higher over 40% HPW-Al-MCM-41 (50) than over 20% HPW-Al-MCM-41 (50) at 60, 80, 100 and 120 °C. The high conversion over 40% HPW-Al-MCM-41 (50) is ascribed to the formation of Lewis acid sites by the reaction between HPW and Al-MCM-41 (50) and the uniform dispersion of HPW on Al-MCM-41 (50) [27]. Usha Nandhini et al. [12] reported generation of Lewis acid sites as a result of HPW loading on Al-MCM-41 (50). Hence Lewis acid sites of both HPW and Al-MCM-41 are the active sites for catalysing the reaction. The epoxidation of maleic acid has been reported over sodium tungstate which bears only Lewis acid sites [28]. Hence the reaction required mainly Lewis acid sites for adsorption and activation of TBHP in order to epoxidise DMM.

The conversion over 20% HPW-Hβ zeolite is close to 40% HPW-Al-MCM-41 (50). Hence there may be more dispersion of active sites in the former than the latter. The absence of Keggin phase in the XRD pattern is an evident for such assumption. As a result it could be visualized that the available Lewis acid sites of HPW and the support may be almost the same in both the catalysts. The activity of Hβ zeolite is close to 20% HPW-Al-MCM-41 (50). Since Lewis acid sites alone catalyse this reaction, Hβ zeolite is expected to possess as many available Lewis sites as 20% HPW-Al-MCM-41 (50). In other words, there may be more number of defective aluminium sites in Hβ. The activity of 40% HPW-Hβ is only 10% higher than 20% HPW-Hβ. The selectivity of CEMS over 20% HPW-Al-MCM-41 (50) decreases with increase in reaction time due to its conversion to DMT. This observation is also noticed over other catalysts. The high selectivity of CEMS illustrates its resistance to hydrolysis under the reaction conditions. As the acid sites of HPW are strong, CEMS could undergo rapid hydrolysis. But the water present in the reaction mixture is not adequate enough to enhance the hydrolysis of CEMS. When the temperature increases from 60 to 80 °C, the selectivity of CEMS decreases. The same trend of decrease in selectivity with increase in reaction time is also observed at 80 °C. When the reaction temperature is raised to 100 and 120 °C, selectivity of CEMS decreases with increase of reaction time. The selectivity of CEMS over 40% HPW-Al-MCM-41 (50) exhibits similar trend as observed over 20% HPW-Al-MCM-41 (50). Although HPW-Hβ zeolite also exhibits similar trend, the selectivity of CEMS is found to be higher than that obtained over HPW-Al-MCM-41 (50) catalyst. The small pore size of Hβ restricts HPW agglomeration which may be the cause for higher activity over HPW-Hβ zeolite. The activity over Hβ without HPW is not adequate enough for comparison. It is concluded that the optimum temperature for epoxidation of DMM is 80 °C, and 40% HPW-Hβ zeolite is more active than other catalysts. In order to detect any leaching of HPW from the support, a portion of the reaction mixture after 12 h was tested by ICP-MS which proved absence of HPW leaching.

3.6.2. Effect of feed ratio

The effect of feed ratio on conversion and products selectivity was carried over 40% HPW-Hβ zeolite at 80 °C and the results are presented in Table 2. The conversion increases with increase in time at each feed ratio. The conversion increases with increase in TBHP content in the feed for each reaction time. Since the reaction requires chemisorption and activation of TBHP on the catalyst surface, an increase in the TBHP content could facilitate more chemisorption of it. The increase in conversion also suggests availability of residual Lewis acid sites for chemisorption. There is enhanced conversion even at a feed ratio 1:10 suggesting only partial accommodation of TBHP on the active sites at low feed ratios. Irrespective of the feed ratio, CEMS is formed predominately than DMT with selectivity of DMT less than 10%. The selectivity of CEMS increases with increase in reaction time at each feed ratio. However, the selectivity attains more than 90% at a feed ratio 1:2 and it remains the same at 1:5 and 1:10. Since the conversion is more than 80% at 1:2 feed ratio, this feed ratio is taken as the optimum one. Though the conversion is higher at 1:5 and 1:10 than

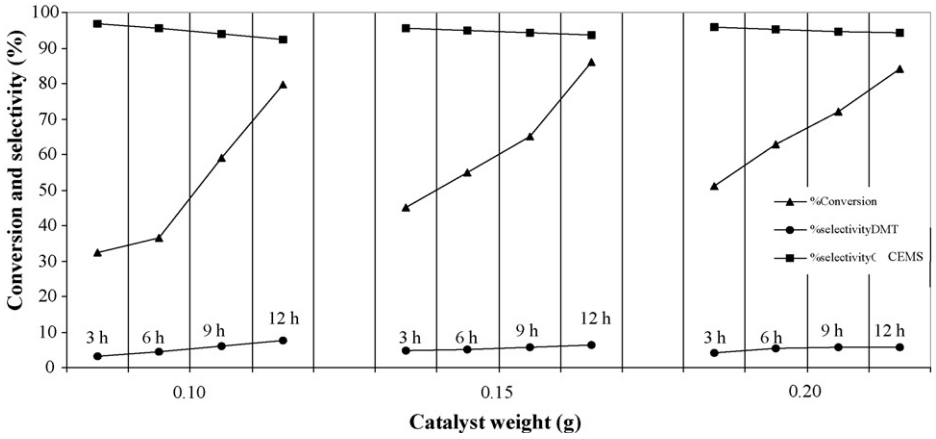

Fig. 6. Effect of catalyst weight on the conversion of DMM and selectivity of products: temperature 80 °C; feed ratio 1:2; catalyst 40% HPW-Hβ.

Table 2
Effect of feed ratio on conversion and products selectivity

Feed ratio	Time (h)	Conversion (%)	Selectivity (%)	
			CEMS	DMT
1:1	3	32.3	29.1	3.2
	6	36.6	32.3	4.3
	9	58.9	52.8	6.1
	12	79.7	72.2	7.5
1:2	3	35	95.2	4.8
	6	40	94.9	5.1
	9	70	94.4	5.6
	12	82	93.8	6.2
1:5	3	45	95.1	4.9
	6	45.3	94.5	5.5
	9	75.2	94.4	5.6
	12	71.3	94.3	5.7
1:10	3	79	94.8	5.2
	6	82	94.5	5.5
	9	91	94.3	5.7
	12	95	93.5	6.5

Temperature: 80 °C; catalyst: 40% HPW-Hβ zeolite; catalyst weight: 0.10 g.

1:2, they are not considered as optimum as they require more TBHP.

3.6.3. Effect of catalyst weight

Since the reaction depends on the activation of TBHP on the active sites of the catalyst, the effect of catalyst weight on the epoxidation will play an important role. Hence the reaction was studied with different catalyst weight and the results are depicted in Fig. 6. The conversion of DMM increases with increase in catalyst weight from 0.10 to 0.15 g. There is no significant change in the conversion upon further increase in catalyst weight. Hence, it is presumed that adsorption and activation of entire TBHP is nearly completed even with 0.10 g of catalyst loading. Hence the optimum loading of catalyst weight is 0.10 g.

4. Conclusion

The results concluded that 40% HPW-Hβ zeolite is found to be more active than others in the epoxidation of DMM with TBHP as it showed 95% conversion and selectivity. The study also revealed that Lewis sites are the active sites for this reaction. High feed ratios are better than lower ones. The formation of only *cis*-epoxydimethyl succinate without its trans isomer proved that epoxidation is a single step process. Supported catalysts are better than those already reported because only minimum amount of HPW was used in this investigation. Problems like leaching of tungstate from resin and maintaining pH of maleic acid are encountered in the epoxidation of maleic acid using tungstate modified Dowex resin. However, such problems were not encountered in the present study. The important observation of this study is the absence of HPW leaching which suggests possible application of this supported catalyst in industries.

Acknowledgements

The authors gratefully acknowledge the financial support from the Department of Science and Technology (DST) (Sanction No. SR/S1/PC-24/2003), Government of India, New Delhi, for this research work. The authors deeply acknowledge the financial support for creating infrastructural facilities in the Department of Chemistry by Department of Science and technology under FIST programme and University Grants Commission (UGC) under special assistance programme (DRS scheme).

References

[1] G.G. Allan, A.N. Neogi, J. Catal. 16 (1970) 197.
[2] D. Swern, J. Am. Chem. Soc. 69 (1947) 1692.
[3] G.G. Allan, US Patent 3,156,709 (1964).
[4] G.B. Payne, P.H. William, J. Org. Chem. 24 (1950) 54.
[5] Japan Patent 73-394335 (1973).
[6] G.G. Allan, A.N. Neogi, J. Catal. 19 (1970) 256.
[7] A. Bavley, C.J. AnKnoth, US Patent 2,972,595 (1961).
[8] T.W. Campbell, R.N.J. Mc Donald, Polym. Sci., Part A 1 (1963) 2525.
[9] J.S. Beck, J.C. Vartuli, W.J. Roth, M.E. Leonowicz, C.T. Kiesge, K.D. Schmitt, C.T.-W. Chu, D.H. Olson, E.W. Sheppard, S.B. McCullen, J.B. Higgins, J.L. Schelnker, J. Am. Chem. Soc. 114 (1992) 10834.
[10] I.V. Kozhevnikov, A. Sinnema, R.J.J. Jansen, K. Pamin, H. van Bekkum, Catal. Lett. 30 (1995) 241.
[11] V. Kozhevnikov, K.K. Kloetstra, A. Sinnema, H.W. Zhandbergen, H. van Bekkum, J. Mol. Catal. A: Chem. 114 (1996) 287.
[12] K. Usha Nandhini, A. Banumathi, M. Palanichamy, V. Murugesan, J. Mol. Catal. A: Chem. 243 (2006) 183.
[13] E.P. Parry, J. Catal. 2 (1963) 371.
[14] C.A. Emeis, J. Catal. 141 (1993) 347.
[15] E.M. Flanigen, in: J.A. Rabo (Ed.), Zeolite Chemistry and Catalysis, ACS Monograph 171, Washington, DC, 1976, pp. 589–591.
[16] V. Umamaheswari, M. Palanichamy, V. Murugesan, J. Catal. 210 (2002) 367.
[17] W.-Y. Chen, H.-X. Li, M.E. Davis, Microporous Mater. 2 (1993) 17.
[18] J.M. Newsman, M.M.J. Treacy, W.T. Koetsier, C.B. De Gruyter, Proc. R. Soc. London A420 (1988) 375.
[19] M.T. Pope, Heteropoly and Isopoly Oxometalates, Springer-Verlag, Berlin, 1983 .
[20] C. Rocchiccioli-Deltcheff, M. Fournier, R. Frank, R. Thouvenot, Inorg. Chem. 22 (1983) 207.

[21] S. Udayakumar, A. Pandurangan, P.K. Sinha, J. Mol. Catal. A: Chem. 216 (2004) 75.
[22] J.A. Dias, E. Caliman, S.C.L. Dias, A. Paulo, C.P. Thyrso Desouza, Catal. Today 85 (2003) 39.
[23] J.A. Dias, J.P. Osegovic, R.S. Drago, J. Catal. 183 (1999) 83.
[24] A. Corma, Chem. Rev. 95 (1995) 559.
[25] K. Shanmugapriya, M. Palanichamy, B. Arabindoo, V. Murugesan, J. Catal. 224 (2004) 347.
[26] M. Karthik, A. Vinu, A.K. Tripathi, N.M. Gupta, M. Palanichamy, V. Murugesan, Microporous Mesoporous Mater. 70 (2004) 15.
[27] I.V. Kozhevnikov, Appl. Catal. A: Gen. 256 (2003) 3.
[28] K. Hosoi, M. Hashimoto, T. Okuhara, M. Misono, US Patent 4,065,475 (1977).